

Supplementary Information: Reversible stress-induced doping and charge trap generation in IDT-BT EGOFET

Axel Luukkonen,^a Jonas Jern,^a Qiao He,^b Martin Heeney^{b,c}, and Ronald Österbacka^{*a}

^a Åbo Akademi University, Faculty of Science and Engineering, Henrikinkatu 2, Turku

^b Imperial College London, Department of Chemistry and Centre for Processable Electronics, London W12 0BZ, UK

^c KAUST Solar Center (KSC), Physical Sciences and Engineering Division (PSE), King Abdullah University of Science and Technology (KAUST), Thuwal 23955-6900, Saudi Arabia

*E-mail: ronald.osterbacka@abo.fi

† Electronic Supplementary Information (ESI) available: [details of any supplementary information available should be included here]. See DOI: 00.0000/000000

S1: Film thickness measurements

The film thickness was measured on an identically prepared substrate using Atomic Force Microscopy (AFM). Part of the film was removed by submerging half of the substrate in IPA during ultrasonication, resulting in a step over which a thickness profile could be extracted. The data was analyzed using Gwyddion. Figure 1 shows the height channel from the AFM micrograph, levelled in the Y-direction with the step where IDT-BT has been removed clearly visible. Figure 2 shows the height profile along the line in Figure 1. Using this, the film thickness was estimated to 60 nm.

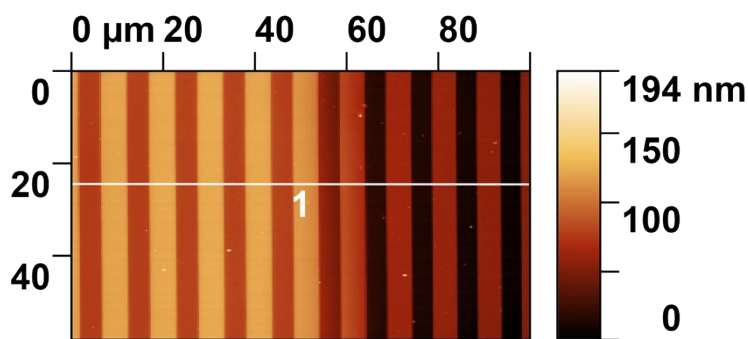


Figure S1: AFM micrograph of Source-Drain finger structure where the IDT-BT layer has been partially removed.

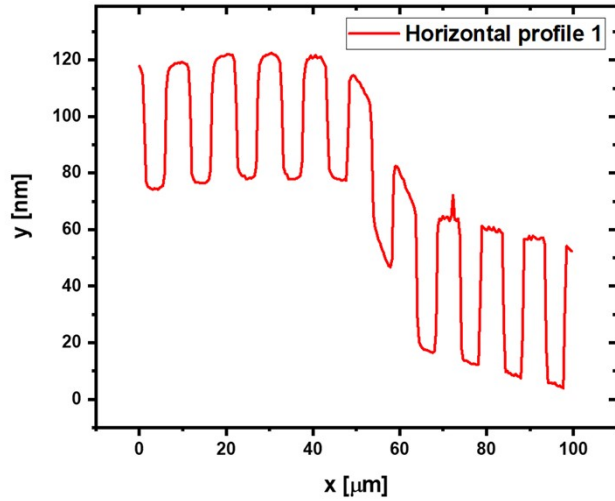


Figure S2: Extracted height profile from AFM micrograph.

S2: Comparison of sweep rates to ensure minimal hysteresis.

Using an identically prepared device to the one in the main text, after overnight stabilization, we investigated the effect of sweep rate on hysteresis. Figure S6 shows subsequent transfer curves measured with different sweep rates. Even at the highest sweep speed of 10 V per second, we observe only minimal hysteresis.

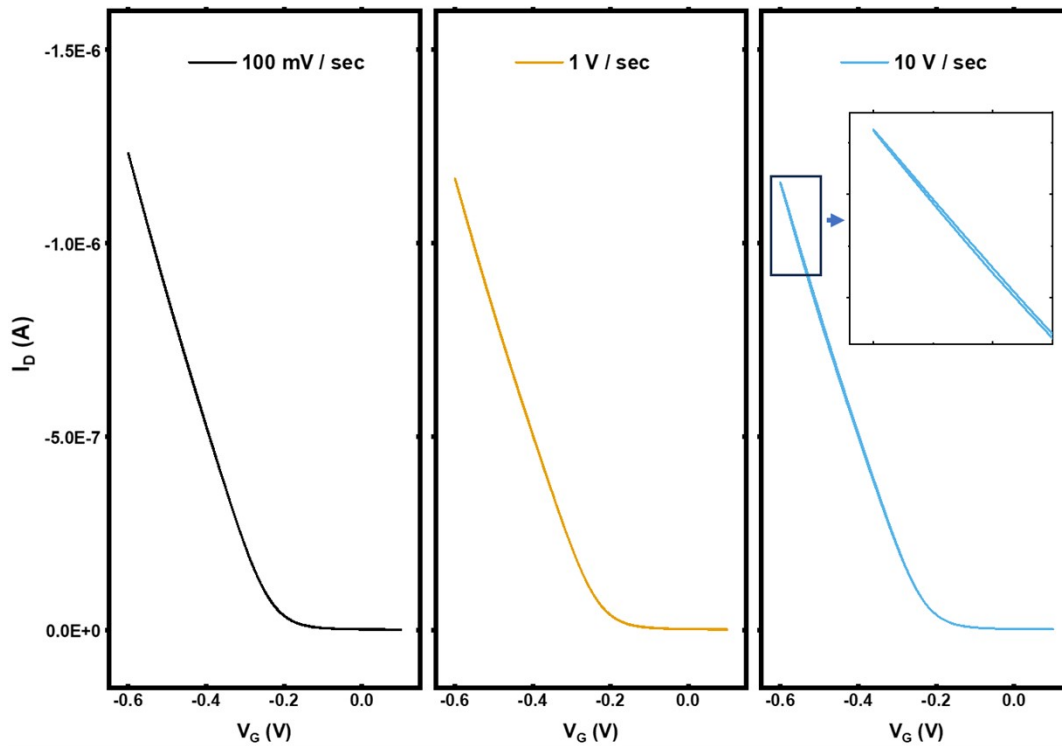


Figure S6: Transfer curves measured at different sweep rates. Some hysteresis is present at the highest sweep rate, but at lower sweep rates the hysteresis is entirely negligible.

S3: Repetition of alternating stress measurement using a different device.

To ensure that the reversible doping is reproducible, the first set of alternating stress measurements (Figure 7 in the main text) were repeated using an identically prepared device from a different batch. Figure S3 shows that the effect is indeed present here as well. Overall, the performance of this particular EGOFET is lower than in the one presented in the main text, as can be seen from the lower mobility and thus lower current. This can likely be attributed to an inferior PFBT SAM functionalization, as this would lead to higher contact resistance. Nonetheless, the reversible doping is clearly present in this device as well.

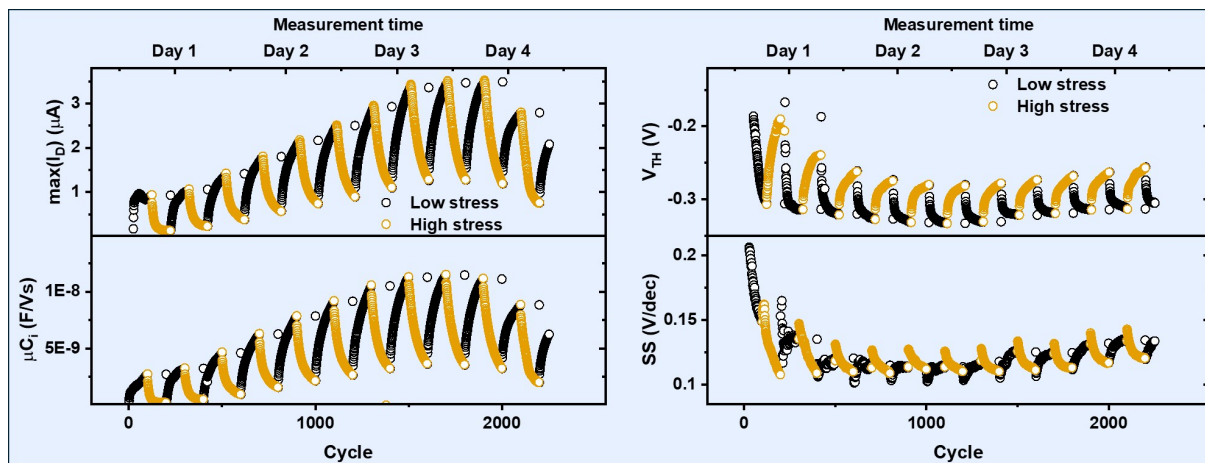


Figure S5: Evolution of the figures of merit during 2250 transfer cycles and four days of EGOFET operation, for an identically prepared device to that presented in the main text. During high stress, the device is biased with $V_D = -0.5$ V and $V_G = -0.6$ V for 120 seconds between each transfer measurement, while during low stress no bias is applied for the same duration between transfer measurements. This figure is analogous to Figure 7 in the main text, but for a device from a different batch.

S4: Transfer curves throughout the device lifetime.

Here we show additional transfer measurement data, illustrating that the device behavior is as illustrated by the figures of merit presented in the main text. The final transfer measurement from each high/low stress series corresponding to the higher and lower doped states, respectively. Figure S3 shows these transfer curves from the first alternating stress measurement series in linear and logarithmic scale, with data from high stress measurements in red scale and data from low stress measurements in blue scale. Figure S4 shows the corresponding transfer curves from the alternating stress measurements performed at higher gate bias.

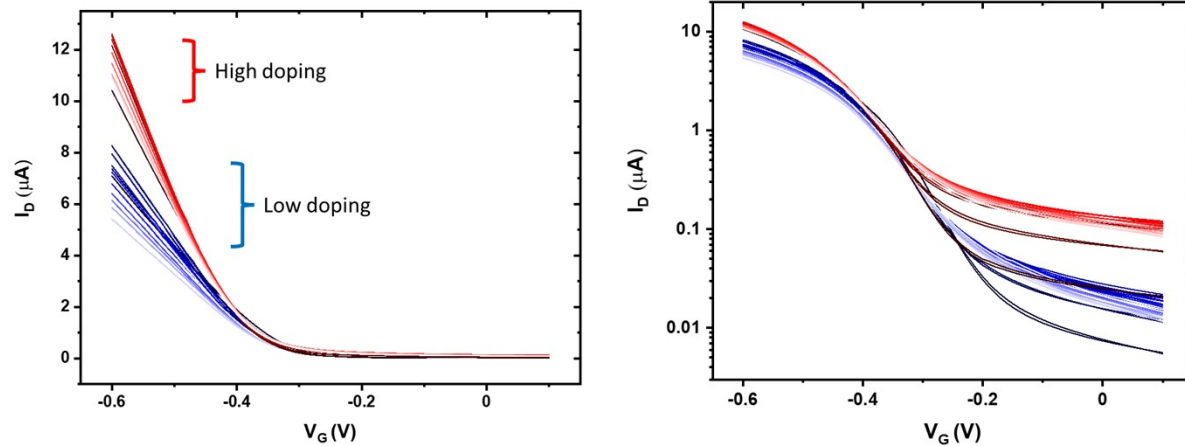


Figure S3: The final transfer measurements in each high/low stress run performed during the first alternating stress measurement series.

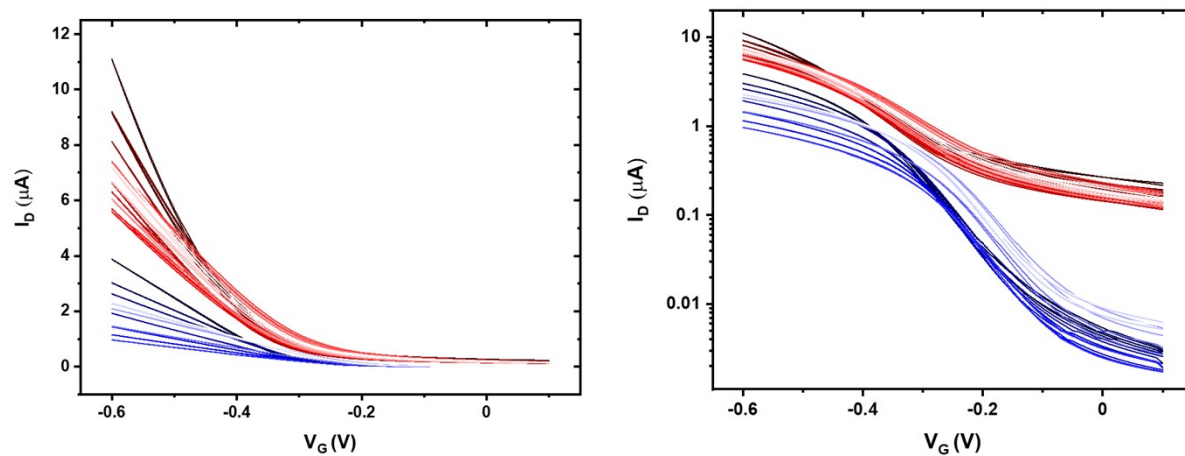


Figure S4: The final transfer measurements in each high/low stress run performed during the alternating stress measurements at higher gate bias.